35th Annual International Conference of the IEEE EMBS
Osaka, Japan, 3 - 7 July, 2013

Advanced Fluorescence Lifetime Imaging Algorithms for CMOS Single-Photon Sensor Based Multi-focal Multi-photon Microscopy

D. D.-U. Li, S. Poland, S. Coelho, D. Tyndall, W. Zhang, J. Richardson, R.K. Henderson, and S.M. Ameer-Beg

***Abstract*— We have developed a fast hardware friendly bi-exponential fluorescence lifetime algorithm suitable for 2D CMOS single-photon avalanche diode (SPAD) arrays. The performance of the proposed algorithm against other techniques is demonstrated on the data from a plant specimen (*Convallaria*) by using 0.13µm CMOS SPAD arrays mounted on a multi-beam multi-photon microscopy system.**

I. Introduction

Fluorescence lifetime imaging microscopy (FLIM) generates images with each pixel sensing the exponential decay rate instead of the intensity of the fluorescence from a fluorophore. It allows imaging different fluorophores with different lifetimes fluorescing at the same wavelength [1, 2]. FLIM, when combining with fluorescence resonance energy transfer (FRET) techniques, called FLIM-FRET hereafter, offer capability of imaging protein-protein interactions in living cells and facilitate scientists to uncover disease mechanisms (such as cancers) in early stage [3]. FRET is a non-radiative process involving transfer of energy from an excited donor fluorophore to an acceptor fluorophore. The FRET efficiency can tell what fraction of donor molecules releases energy to the acceptor, and its dependence on the inverse sixth power of the donor-to-acceptor separation distance making it a powerful ruler to measure protein interactions. When FRET occurs, the excited state population of the donor is depleted reducing the fluorescence lifetime of the donor [4]. The advantage of measuring the fluorescence lifetime of the donor is that lifetime imaging is independent of fluorophore concentration and optical path length. It is therefore well suited to studies in intact cells [3, 4]. In a conventional FLIM experiment, a photomultiplier (PMT) capable of single-photon detection is used in combination with a time-correlated single-photon counting (TCSPC) module in which a high-resolution, but power-hungry time-to-digital converter (TDC) is used to measure the time delay of each detected photon with respect to the laser excitation pulse. The lifetime calculations are carried out, usually using iterative nonlinear Marquardt-Levenberg algorithms on a pixel-by-pixel basis. The drawback of single-channel PMT-TCSPC systems is therefore slow image acquisition and generation. Although multi-channel PMT-TCSPC systems are commercially available, they are expensive and limited to fewer than 16 channels. With recent advances in CMOS technology, PMT-like single-photon detectors can be fabricated in low lost CMOS processes using avalanche diode structures [5]. The MEGAFRAME chip integrates 32x32 low noise SPADs with in-pixel 55ps 10-bit TDCs can act as a 1024-channel miniaturized TCSPC system [5, 6]. The in-pixel TDC is ring oscillator based with low power consumption and a dynamic range of 95ns (resolution = 93ps when PLL is enabled) covering the fluorescent lifetimes of the usual fluorophores used in laboratory microscopy experiments. Each pixel can generate 500k arrival times per second. The maximum data throughput is 32x32x10x500k = 5Gbps. To reduce the data throughput from the camera to a PC, we have implemented several on-FPGA single-exponential FLIM algorithms using integral equation method (IEM) [7] or center-of-mass method (CMM) [8] and successfully demonstrated video-rate wide-field lifetime imaging [9, 10].

FRET occurs only when the donor and acceptor are placed typically within ~10 nm. To achieve enough spatial resolution for FLIM-FRET applications, the MEGAFRAME chip is mounted on a custom multifocal multiphoton microscope (MMM) [11] with novel optical arrangements to focus the fluorescence emission on the active area of the SPADs to improve the fill factor from 2% (due to the in-pixel TDC and memory) to above 50% [12, 13]. There is no need to resort to microlens arrays [14]. Currently 64 pixels out of 1024 are used due to limitations in the number of beamlets generated. Besides the optical development, a new digital architecture for fast acquisition of TCSPC arrival times has also been developed to increase the data transfer rate to 95k count per second (cps) per pixel (= 6.1Mcps in total) [15]. As we continue to optimize the acquisition of the SPAD-MMM system or implement on-chip histograms to reduce the data throughput, the imaging bottleneck will gradually shift from acquisition to lifetime calculation. It still takes a significant amount of time to extract the lifetimes by using iterative-based software [16]. Although our previously developed single-exponential FLIM algorithms are simple and can provide high-speed imaging with enough contrast [9, 10], scientists are keen to visualize the fraction of interacting donors in FRET experiments. A fast algorithm called the minimal fraction of interacting donors was proposed to provide quantitative FRET analysis

*Research supported by the Royal Society and BBSRC (BB/I022074/1 and BB/I022937/1).

D. D.-U. Li and W. Zhang are with the School of Engineering and Informatics, University of Sussex, Brighton BN1 9QT, UK (phone: +44 1273873513; e-mails: David.Li@sussex.ac.uk; wz39@sussex.ac.uk).

S. Poland, S. Coelho and S. Ameer-Beg are with the Richard Dimbleby Department of Cancer Research, King's College London, London SE1 1UL, UK (e-mails: simon.poland@kcl.ac.uk; simon.ameer-beg@kcl.ac.uk; simao.pereira_coelho@kcl.ac.uk).

D. Tyndall and J. Richardson are with the Dialog Semiconductor, Edinburgh EH1 3DQ, Scotland, UK. (e-mails: david.tyndall@diasemi.com; justin.richardson@diasemi.com).

R. K. Henderson is with the the University of Edinburgh, Edinburgh EH9 3JL, Scotland, UK. (e-mail: robert.henderson@ed.ac.uk).

[17], but it is actually a single-exponential method similar to our CMM [10]. In this paper, we will introduce a hardware-friendly bi-exponential FLIM algorithm suitable for our highly parallelized SPAD-TCSPC camera. The formulation and Monte Carlo error analysis of the algorithm will be introduced in Sec. II. Finally, we will test the algorithm off-line on a FLIM image obtained from a plant specimen (*Convallaria*) by the SPAD-MMM system. We will compare the results with other techniques.

II. Theory

A. Parameters Required for Fast Bi-decay FLIM

For simplicity, we consider a bi-exponential decay with a negligible instrumental response function (IRF). Such an assumption allows a proper comparison of various bi-exponential fitting algorithms. The contribution of the IRF has been studied in [7, 18]. We can extend our algorithm by including the contribution of the IRF in the future. Assume the fluorescence decay function $f(t) = [A_1\exp(-t/\tau_1) + A_2\exp(-t/\tau_2)]u(t)$ with τ_1, τ_2 being the lifetimes, A_1, A_2 the pre-scalars and $u(t)$ the step function. We also neglect the background noise as recent developments of CMOS SPADs have shown significant improvements in the dark count rate [5, 19-21]. Unlike conventional TCSPC systems sending all raw arrival time data to a PC for post-processing, it is possible to *pre-process* some data with minimum extra electronics hardware. The parameters we can record to extract A_1, A_2, τ_1 and τ_2 are (1) the photon count in the first bin, N_1, (2) the total photon count, N_C, (3) the sum of all arrival times, X_1, and (4) the sum of all squared arrival times, X_2. Assume the resolution of the in-pixel TDC is h, we can extract τ_1, τ_2, A_1, and A_2, from the above four constraints as

$$\tau_1 = \frac{S - \sqrt{S^2 - 4(N\cdot S - X_1)/K}}{2}, \quad (1)$$

$$\tau_2 = \frac{S + \sqrt{S^2 - 4(N\cdot S - X_1)/K}}{2}, \quad (2)$$

$$A_1 = \frac{K\cdot\tau_2 - N}{\Delta\tau}, \quad (3)$$

$$A_2 = \frac{N - K\cdot\tau_1}{\Delta\tau}, \quad (4)$$

$$S = \frac{K\cdot X_2 - 2N\cdot X_1}{K\cdot X_1 - 2N^2}, \quad (5)$$

$$X_1 = \sum_{j=1}^{N_C} t_j, \; X_2 = \sum_{j=1}^{N_C} t_j^2, \quad (6)$$

with t_j (j = 1,…, N_C) being the arrival time of the j^{th} photon, $K = N_1/h$ and $\Delta\tau = \tau_2 - \tau_1$. Equations (1)-(4) contain no iterative operation, so the lifetime calculation is much faster than the iterative nonlinear Marquardt-Levenberg algorithm. Without using any logarithmic function, the calculation is quicker than the fast multi-gate algorithm proposed by Sharman and Periasamy [22, 23]. As the accumulators for storing N_1, N_C, X_1 and X_2 can be implemented on-chip or on-FPGA, they can easily operate at frequencies over several MHz. For biologists who prefer detailed analysis using global analysis software, we can also build on-FPGA histogram builders and send data off-line. The proposed algorithm is denoted as Adv. CMM hereafter for its resemblance to our previously developed CMM [9].

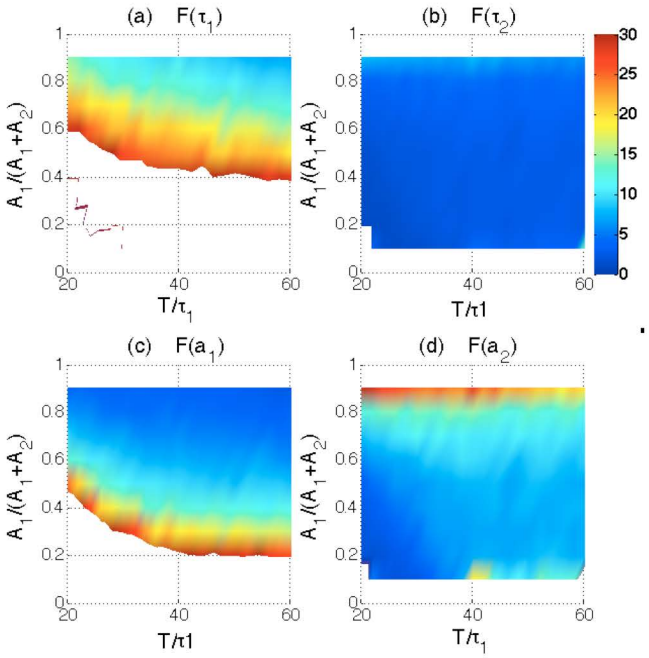

Figure 1 (a) F-value plots for A_1, A_2, τ_1 and τ_2.

B. Monte Carlo Simulations

To use the Adv. CMM properly, deriving the error equation is essential as users can apply a proper measurement setting to optimize the imaging performance. Due to the publication length limit, we will skip the theoretical derivations and use Monte-Carlo simulations to do the error analysis. Figures 1 (a)-(d) show the F-value precision plots (F is defined in [24]. $F \equiv N_C^{0.5}\delta g/g$, $g = A_1$, A_2, τ_1 and τ_2, F = 1 for the ideal case) of Adv. CMM for $\tau_2/\tau_1 = 4$ (this ratio is close to the data we will analyze in the Experimental Results section). It is interesting that in some situations the A_1 and A_2 images can provide more precise imaging than the τ_1 images, as the local relative variations of A_1 and A_2 are smaller. The τ_2 images are generally less sensitive to the measurement settings and can provide the best precision.

III. Experimental Results

A. SPAD-MMM Setup

Figure 2 (a) shows the SPAD camera assembly carrying a new spun uniform TDC array different from the previous version [6]. Underneath the assembly sits an Opal Kelly XEM3050 FPGA (Xilinx Spartan3 XC3S4000) board. The board has an USB2 module. The full width half maximum (FWHM) of the SPAD pixels is around 300ps. The SPAD-MMM system is shown in Fig. 2(b), in which the spatial light modulator is used to generate the required 2D laser beamlets. The patterned light is directed through a set of x and y galvanometer scanners, relay lenses, a dichroic mirror and shined on the sample via the Nikon x20, 0.5NA air objective,

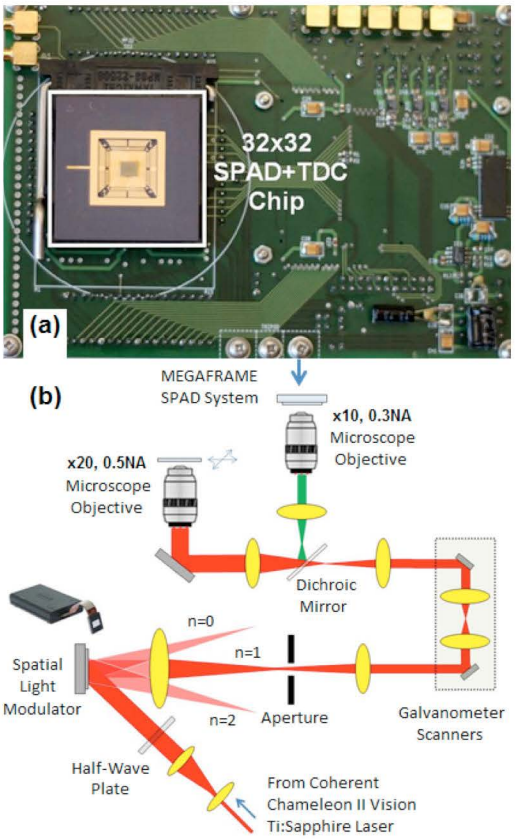

Figure 2 (a) SPAD camera assembly and (b) multifocal multiphoton microscope setup.

whereas the two photon fluorescent emission is collected by the objective and is directed by the dichroic mirror onto the MEGAFRAME chip via another Nikon x10 0.3NA air objective [12, 13].

B. Results and Discussion

To test the proposed algorithm, a multibeam multiphoton sample scan was performed with 8×8 beamlets at the excitation wavelength of 800nm on a thin section of Convallaria Majalis (lily of valley). The 2D beamlets can produce a 256×256 FLIM image with each beamlet scanning 32×32 points. Figures 3(a)-(d) show the τ_1, τ_2, A_1 and A_2 images obtained by Adv. CMM respectively using the data acquired by the SPAD-MMM in 20s. The images show the auto-fluorescence lifetime information was captured by the SPAD chip and can be resolved by Adv. CMM. Unlike single-exponential models only providing lifetime information, the magnitudes of different fluorescence emissions are also revealed. In FRET experiments, it is the fraction of interacting donors or acceptors showing how proteins interact. Fig. 3(e) shows the fluorescence intensity, and Fig. 3(f) is the intensity-weighted average lifetime image, which actually matches our previously proposed CMM [9, 25]. We can also apply the fast multi-gate bi-exponential model in the SPAD system as the model allows using only four counters to store the photon counts. The fast gating model, however, is sensitive to noise. Also, the formulation contains logarithmic functions, which often generate complex numbers if the photon count is not big enough. For example, Adv. CMM generates about 15000 valid lifetimes, whereas the fast multi-gate model generates ~11000 valid lifetimes (a threshold count of 140 is applied). Figs 3(g) and (h) also show bigger variations indicating longer acquisition

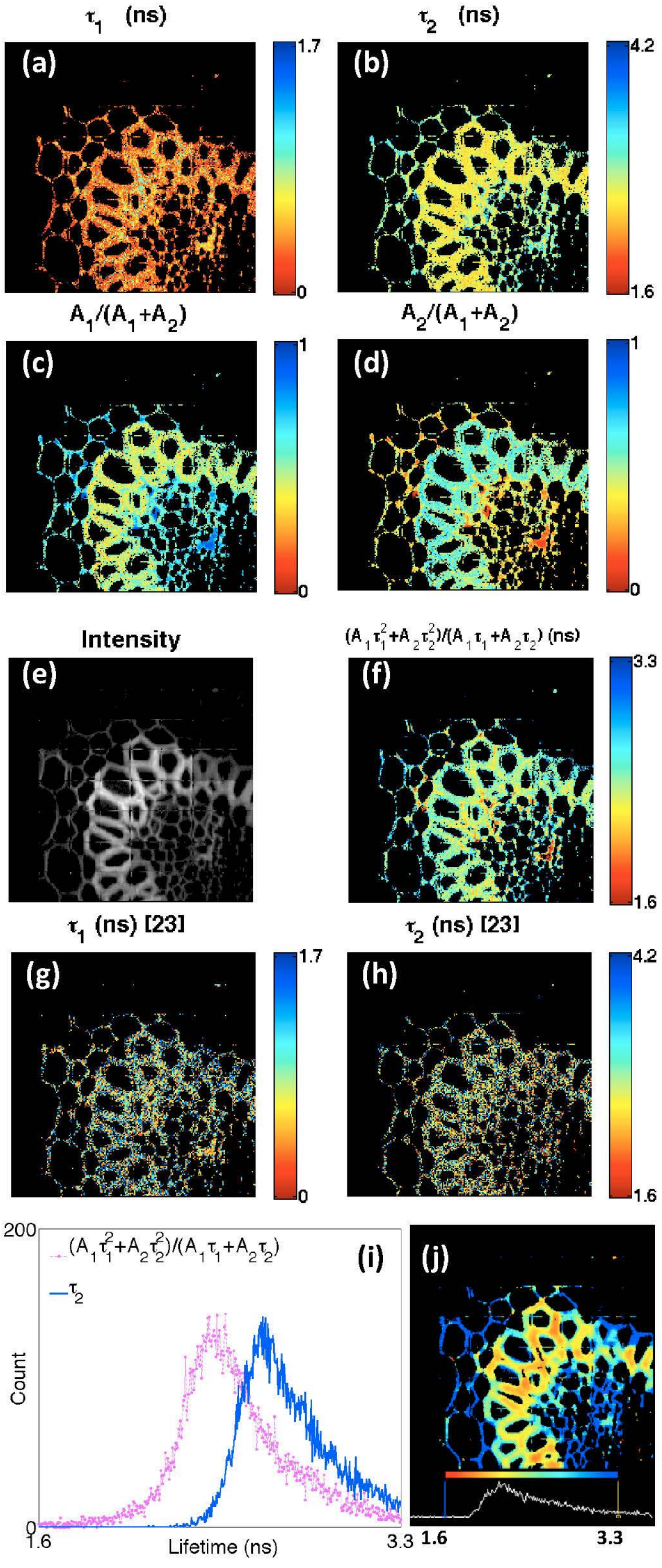

Figure 3. (a)-(d) τ_1, τ_2, A_1 and A_2 images obtained by Adv. CMM. (e) Fluorescence intensity image, (f) intensity-weighted average lifetime image obtained by Adv. CMM, (g)-(h) τ_1 and τ_2 images obtained by fast multi-gate method [23], (i) lifetime histograms and (j) intensity-weighted lifetime map and histogram obtained by the TRI2 software.

TABLE I. CALCULATED LIFETIMES USING ADV. CMM AND MULTI-GATE BI-DEAY MODEL [23]

	Eqs (1) – (5)	Multi-Gate Bi-decay
τ_1	0.4 ± 0.20 ns	1.0 ± 0.39 ns
τ_2	2.8 ± 0.25 ns	3.3 ± 1.10 ns

is required for the multi-gate model to guarantee enough accuracy. Table I shows the calculated lifetimes obtained by using Adv. CMM and the multi-gate bi-exponential model [23]. In terms of accuracy, Adv. CMM provides better τ_2 imaging with a comparable precision for τ_1 imaging with the multi-gate model probably due to the contribution of the IRF. From Figs. 3 (f), (i) and (j), Adv. CMM provides a comparable lifetime image and histogram for the intensity-weighted average lifetime with the TRI2 software [16].

IV. CONCLUSION

We have proposed a fast bi-exponential FLIM algorithm suitable for the recently developed CMOS SPAD-MMM system. As the acquisition speed and data transfer have been enhanced and efforts are put to optimize the beamlet generation algorithms, the proposed hardware-friendly bi-exponential FLIM algorithm can help relieve the bottleneck caused by the lifetime calculation showing great potential in future FLIM-FRET applications. The algorithm can be implemented on-chip to compress the data from the sensor arrays. It can be also implemented in an FPGA chip to reduce the throughput between the camera system and a PC or even in software. Further study will be carried out to investigate a proper implementation scheme. Without using any iteration, the proposed algorithm has great potential to visualize protein-protein interactions in real-time.

ACKNOWLEDGMENT

The authors would like to thank the Royal Society and the BBSRC (BB/I022074/1 and BB/I022937/1) for their support and the STMicroelectronics, Edinburgh for manufacturing new MEGAFRAME SPAD chips. We would like to thank Nikola Krstajic and Richard Walker for designing the SPAD acquisition systems. We would also like to thank the Cancer Research UK for their support to the KCL/UCL Comprehensive Cancer Imaging Centre.

REFERENCES

[1] F.S. Wouters and P.I. Bastiaens, "Fluorescence lifetime imaging of receptor tyrosine kinase activity in cells," Curr. Biol., vol. 9, pp. 1127-1130, 1999.

[2] W. Becker, "Fluorescence lifetime imaging – techniques and applications," J. Microsc., vol. 247, pp. 119-136, 2012.

[3] L.M. Carlin, *et al*., "A targeted siRNA screen identifies regulators of Cdc42 activity at the Natural Killer cell immunological synapse," Science Signalling, vol. 4, p. ra81, 2011.

[4] Y. Sun, R. N. Day, and A. Periasamy, "Investigating protein-protein interactions in living cells using fluorescence lifetime imaging microscopy, Nature Protocols, vol. 6, pp.1324-1340, 2011.

[5] J. A. Richardson, L.A. Grant, and R.K. Henderson, "Low dark count single-photon avalanche diode structure compatible with standard nanometer scale CMOS technology," IEEE Photon. Tech. Lett., vol. 21, pp. 1020-1022, 2009.

[6] J. A. Richardson, R. Walker, L. Grant, D. Stoppa, F. Borghetti, E. Charbon, M. Gersbach, and R.K. Henderson, "A 32x32 50ps resolution 10-bit time-to-digital converter array in 130nm CMOS for time correlated imaging," Proc. IEEE Custom Integrated Circuits Conf. (CICC), San Jose, CA, 13-16 Sept. 2009, pp. 77-80.

[7] D.-U. Li, E. Bonnist, D. Renshaw, and R. Henderson, "On-chip time-correlated fluorescence lifetime extraction algorithms and error analysis," J. Opt. Soc. Am. A, vol. 25, pp. 1190-1198, 2008.

[8] D.-U. Li, B. Rae, R. Andrews, J. Arlt and R. Henderson, "Hardware implementation algorithm and error analysis of high-speed fluorescence lifetime sensing systems using center-of-mass method, J. Biomed. Opt., vol. 15, 017006-1-017006-10, 2010.

[9] D.-U. Li, J. Arlt, J. Richardson, R. Walker, A. Buts, D. Stoppa, E. Charbon, and R. Henderson, "Real-time fluorescence lifetime imaging system with a 32x32 0.13μm CMOS low dark-count single-photon avalanche diode array," Opt. Express, vol. 18, pp. 10257-10269, 2010.

[10] D. D.-U. Li, J. Arlt, D. Tyndall, R. Walker, J. Richardson, D. Stoppa, E. Charbon and R. Henderson, "Video-rate fluorescence lifetime imaging camera with CMOS single-photon avalanche diode arrays and high-speed imaging algorithm," J. Biomed. Opt., vol. 16, 096012-1-096012-12, 2011.

[11] J. Bewersdorf, R. Pick, and S.W. Hell, "Multifocal multiphoton microscopy," Opt. Lett., vol. 23, pp. 655-657, 1998.

[12] S. Poland, S. Coelho, N. Krstajic, D. Tyndall, R. Walker, D. D.-U. Li, R. Henderson, and S. Ameer-Beg, "Development of a fast TCSPC FLIM-FRET imaging system," Proc. SPIE, to be published.

[13] S. Coelho, S. Poland, N. Krstajic, D. D.-U. Li, R. Henderson, and S. Ameer-Beg, "Multibeam multiphoton microscopy with adaptive optical correction," Proc. SPIE, to be published.

[14] C. Veerappan, J. Richardson, R. Walker, D.-U. Li, M.W. Fishburn, Y. Maruyama, D. Stoppa, F. Borghetti, M. Gersbach, R.K. Henderson, and E. Charbon, "A 160x128 single-photon image sensor with on-pixel 55ps 10bit time-to-digital converter," Proc. IEEE Int. Solid-State Circuits Conference (ISSCC), San Francisco, Feb. 2011, pp. 312-314.

[15] N. Krstajic, S. Poland, D. Tyndall, R. Walker, S. Coelho, D. D.-U. Li, J. Richardson, S. Ameer-Beg, and R. Henderson, "Improving TCSPC data acquisition from CMOS SPAD arrays," submitted to 2013 European Conferences on Biomedical Optics (ECBO) for publication.

[16] P.R. Barber, *et al*., "Multiphoton time-domain fluorescence lifetime imaging microscopy: practical application to protein-protein interactions using global analysis," J. R. Soc. Interface, vol. 6, S93-S105, 2009.

[17] S. Padilla-Parra, N. Auduge, M. Coppey-Moisan, and M. Tramier, "Quantitative FRET analysis by fast acquisition time domain FLIM at high spatial resolution in living cells," Biophys. J., vol. 95, pp. 2976-2988, 2008.

[18] J.A. Jo, Q. Fang, T. Papaioannou, and L. Marcu, "Novel ultra-fast deconvolution method for fluorescence lifetime imaging microscopy based on the Laguerre expansion technique," Proc. 26th Annual International Conference of the IEEE EMBS (EMBC), San Francisco, CA, 1-5 September 2004, pp. 1271-1274.

[19] E.A.G. Webster, L.A. Grant, and R. Henderson, "A high-performance single-photon avalanche diode in 130nm CMOS imaging technology," IEEE Electron. Device Lett., vol. 33, pp. 1589-1591, 2012.

[20] F.-Z. Hsu, J.-Y. Wu, and S.-D. Lin, "Low-noise single-photon avalanche diodes in 0.25μm high-voltage CMOS technology," Opt. Lett., vol. 38, pp. 55-57, 2013.

[21] S. Mandai, M.W. Fishburn, Y. Maruyama, and E. Charbon, "A wide spectral range single-photon avalanche diode fabricated in an advanced 180nm CMOS technology," Opt. Express, vol. 20, pp. 5849-5857, 2012.

[22] KK. Sharman and A. Periasamy, "Error analysis of the rapid lifetime determination method for double-exponential decays and new windowing schemes," Ana. Chem., vol. 71, pp. 947-952, 1999.

[23] M. Elangovan, R.N. Day, and A. Periasamy, "A nanosecond fluorescence resonance energy transfer fluorescence lifetime imaging microscopy to localize the protein interactions in a single living cell," J. Microsc., vol. 205, pp. 3-14, 2002.

[24] A. Draaijer, R. Sanders, and H.C. Gerritsen, "Fluorescence lifetime imaging, a new tool in confocal microscopy," in Handbook of Biological Confocal Microscopy, J. Pawley, Ed., pp. 491-505, Plenum Publishing, New York, 1995.

[25] D.D.-U. Li, S. Ameer-Beg, J. Arlt, D. Tyndall, R. Walker, D.R. Matthews, V. Visitkul, J. Richardson, and R.K. Henderson, "Time-domain fluorescence lifetime techniques suitable for solid-state imaging sensor arrays," Sensors, vol. 12, pp. 5650-5669, 2012.